Biochemical and Biophysical Research Communications 429 (2012) 63–69

Contents lists available at SciVerse ScienceDirect

Biochemical and Biophysical Research Communications

journal homepage: www.elsevier.com/locate/ybbrc

Recombinant expression and solution structure of antimicrobial peptide aurelin from jellyfish *Aurelia aurita* ☆

Zakhar O. Shenkarev [a], Pavel V. Panteleev [a], Sergey V. Balandin [a], Albina K. Gizatullina [a,b], Dmitry A. Altukhov [a,b], Ekaterina I. Finkina [a], Vladimir N. Kokryakov [c], Alexander S. Arseniev [a,b], Tatiana V. Ovchinnikova [a,b,*]

[a] *Shemyakin and Ovchinnikov Institute of Bioorganic Chemistry, Russian Academy of Sciences, Miklukho-Maklaya str., 16/10, 117997 Moscow, Russia*
[b] *Moscow Institute of Physics and Technology (State University), Department of Physicochemical Biology and Biotechnology, Institutskii per., 9, 141700 Dolgoprudny, Moscow Region, Russia*
[c] *Institute of Experimental Medicine, Russian Academy of Medical Sciences, Academica Pavlova str., 12, 197376 Saint-Petersburg, Russia*

ARTICLE INFO

Article history:
Received 15 October 2012
Available online 5 November 2012

Keywords:
Antimicrobial peptide
Aurelin
Aurelia aurita
Recombinant expression
NMR
Spatial structure

ABSTRACT

Aurelin is a 40-residue cationic antimicrobial peptide isolated from the mezoglea of a scyphoid jellyfish *Aurelia aurita*. Aurelin and its ^{15}N-labeled analogue were overexpressed in *Escherichia coli* and purified. Antimicrobial activity of the recombinant peptide was examined, and its spatial structure was studied by NMR spectroscopy. Aurelin represents a compact globule, enclosing one 3_{10}-helix and two α-helical regions cross-linked by three disulfide bonds. The peptide binds to anionic lipid (POPC/DOPG, 3:1) vesicles even at physiological salt concentration, it does not interact with zwitterionic (POPC) vesicles and interacts with the DPC micelle surface with moderate affinity via two α-helical regions. Although aurelin shows structural homology to the BgK and ShK toxins of sea anemones, its surface does not possess the "functional dyad" required for the high-affinity interaction with the K^+-channels. The obtained data permit to correlate the modest antibacterial properties and membrane activity of aurelin.

1. Introduction

Endogenous antimicrobial peptides (AMPs) of animal origin are evolutionarily conserved and ubiquitous molecules involved in innate defense mechanisms of a wide range of organisms protecting them against a broad repertoire of pathogenic bacteria, fungi, protozoa, and enveloped viruses [1]. Marine invertebrates lack an acquired immunity with a system of antibody diversification and rely solely on innate immune mechanisms. The survival of marine invertebrate animals in microbe-laden environment suggests that their innate immune system is effective and robust. AMPs are a major component of the innate immune defense system in marine invertebrates [2]. They are defined as peptide molecules which exhibit antimicrobial properties and provide an emergent response to invading microorganisms. Despite an impressive variety of already discovered and characterized marine invertebrate AMPs [3], mechanisms of their antimicrobial action are still obscure. As marine invertebrates AMPs are considered potential peptide antibiotics for combating microbial drug resistance, their structures and mode of action need deeper analysis.

From a structural point of view, AMPs demonstrate high diversity [1]. However, all these peptides (including α-helical peptides, β-structural disulfide-rich peptides, and the peptides without segments of defined secondary structure) share common structural properties: they contain large portion of cationic and hydrophobic amino acid residues, form amphipathic structures upon contact with lipid membranes, and demonstrate significant membrane activity [1,4]. This activity of AMPs is believed to be either the main mode of their action resulting in membrane disruption and cell lysis, or an intermediate step promoting AMPs penetration to intracellular targets [4]. It is generally assumed that the overall positive charge underlies AMPs selectivity towards anionic membranes of bacterial cells [5]. The electrostatic peptide/membrane interactions can be significantly weakened upon increase in ionic strength, thus leading to loss in AMPs activity and selectivity even at physiological conditions [6].

Abbreviations: 16-DSA, 16-doxylstearate; DOPG, 1,2-dioleoyl-sn-glycero-3-phosphoglycerol; DPC, dodecylphosphocholine; D:P, detergent to peptide molar ratio; ε, paramagnetic enhancement of transverse relaxation (R_2); Kv, voltage-gated K^+-channel; POPC, 1-palmitoyl-2-oleoyl-sn-glycero-3-phosphocholine; POPG, 1-palmitoyl-2-oleoyl-sn-glycero-3-phosphoglycerol; R_H, hydrodynamic Stokes radius; SUV, small unilamellar vesicles.

☆ The atomic coordinates and structure factors have been deposited in the Worldwide Protein Data Bank (PDB: 2LG4).

* Corresponding author at: Shemyakin and Ovchinnikov Institute of Bioorganic Chemistry, Russian Academy of Sciences, Miklukho-Maklaya str., 16/10, 117997 Moscow, Russia. Fax: +7 495 336 43 33.
E-mail address: ovch@ibch.ru (T.V. Ovchinnikova).

0006-291X/$ - see front matter © 2012 Elsevier Inc. All rights reserved.
http://dx.doi.org/10.1016/j.bbrc.2012.10.092

Marine animals also produce other classes of peptide molecules. The most pharmacologically important of them are toxins which selectively block or modulate membrane receptors and ionic channels [7]. Similarly to AMPs, peptide toxins of marine invertebrates demonstrate a large diversity of structural folds, but mainly they represent compact disulfide-rich molecules. The high affinity and selectivity of toxin/receptor interaction are conditioned by specific functional groups having a definite location on the surface of toxin molecule [8].

AMPs and toxins of evolutionary distant organisms often share similar scaffolds which might be a consequence of divergent evolution from a common ancestor. Earlier, we discovered a novel 40-residue cationic antimicrobial peptide aurelin, exhibiting activity against Gram-positive and Gram-negative bacteria [9]. Aurelin was purified from the mezoglea of a scyphoid jellyfish *Aurelia aurita*. Aurelin has six cysteines forming three intramolecular disulfide bridges (Fig. 1A) and shows a moderate degree of homology (40% and 27.5%, respectively) with K^+-channels blocking toxins BgK [10] and ShK [11] of sea anemones. These toxins are composed of 35–37 amino acid residues and adopt so-called "helical cross-like motif", which encompasses two or three helical elements cross-linked by three disulfide bridges with the C1–C6, C2–C4, C3–C5 arrangement [12] (Fig. 1A and B). According to mutagenesis data, the pair of positively charged and aromatic/hydrophobic residues (Lys-Tyr in case of BgK and ShK), so-called "functional dyad", represents one of the major structural determinants of the toxins high-affinity binding to the external vestibule of Kv channels [8,10,13]. It was proposed that a positively charged side chain of Lys residue directly occludes the ion channel pore upon complex formation [14]. Aurelin possesses the critical Lys28 at a homologous position, but the following Tyr residue is substituted by Leu29.

A homologous six-cysteine motif, termed ShKT domain (SMART database) or "CRISP domain-like" fold (SCOP database) was identified in a number of vertebrate and invertebrate proteins (Fig. 1A), particularly in secreted mucin-like glycoproteins [15], matrix metalloproteases (MMPs) [16], and cysteine-rich secretory proteins (CRISPs) [17,18]. Although the domain function within large proteins is still obscured, it was speculated to be involved in extracellular and intracellular proteins interaction, acting as a signaling ligand or even as an ionic channel-blocking unit [16–18].

In the present work, the bacterial expression system for production of the recombinant aurelin and its ^{15}N-labeled analogue was developed to determine the peptide three-dimensional structure and investigate the mechanisms of its action. Antimicrobial activity, spatial structure, backbone dynamics and interaction of aurelin with lipid vesicles and membrane mimicking detergent micelles were studied.

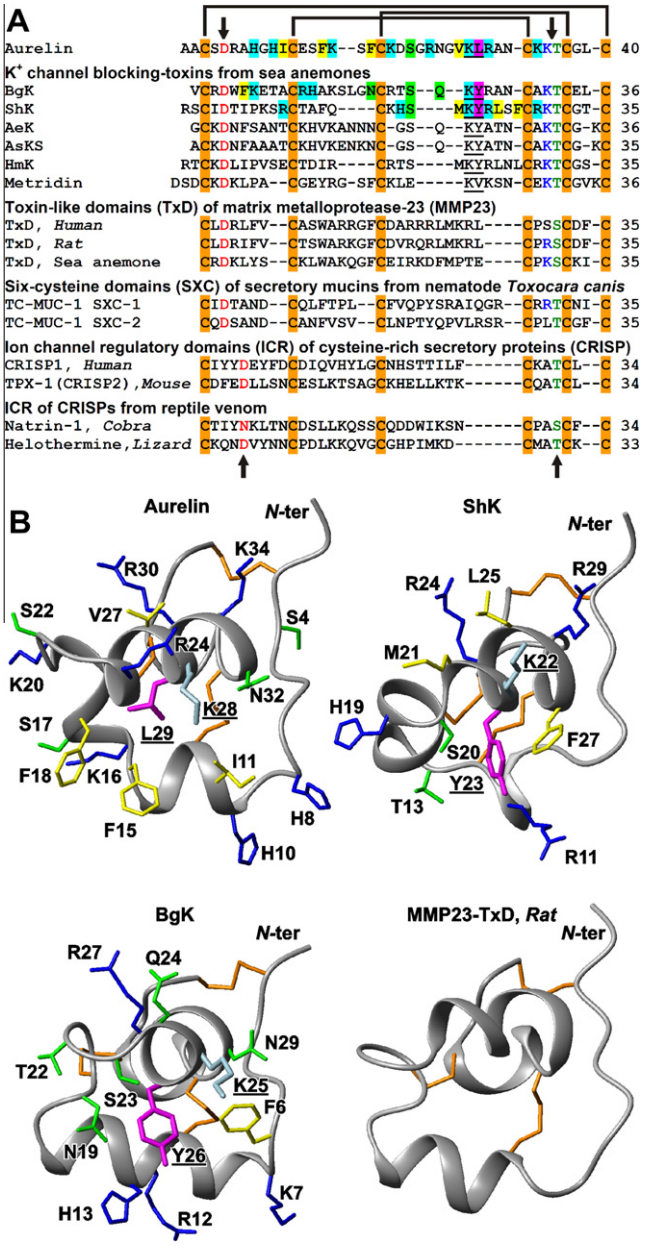

Fig. 1. (A) Amino acid sequence alignment of aurelin [9], K^+-channel blocking toxins from sea anemones [12], toxin-like domains (TxDs) of matrix metalloprotease-23 (MMP23) [16], six-cysteine domains (SXCs) of secretory mucins from nematode *Toxocara canis* [15], ion channel regulatory domains (ICRs) of mammalian cysteine-rich secretory proteins (CRISPs) [17], and ICRs of CRISPs from reptile venom [18]. (B) Comparison of spatial structures of aurelin, ShK, BgK, and MMP23-TxD from rat (PDB codes are 2LG4, 1ROO, 1BGK, and 2K72, respectively). Amino acid residues of BgK and ShK important for binding to Kv channels [8,10,13,14] and the corresponding residues of aurelin are shown. The residues belonging to "functional dyad" are underlined and colored in cyan and magenta. Disulfide bonds, aromatic/hydrophobic, positively charged and other polar residues are colored in orange, yellow, blue, and green, respectively. On the panel A the conservative residues from the Asp/Lys-Thr motif are marked by arrows and highlighted by color. (For interpretation of the references to color in this figure legend, the reader is referred to the web version of this article.)

2. Materials and methods

2.1. Plasmid construction and heterologous expression in Escherichia coli

The recombinant plasmid pET-His8-TrxL-Aur was constructed by ligating the 5253 bp BglII/XhoI fragment of pET-31b(+) vector (Novagen) with a PCR-constructed insert containing the T7 promoter, the ribosome binding site and the sequence encoding the recombinant protein. The last one included octahistidine tag, TrxL carrier protein (*E. coli* thioredoxin A amplified from pET-32a(+) vector (Novagen) in which the M37L mutation was introduced), methionine residue and the mature aurelin (Fig. S1). The sequence coding mature aurelin was amplified from the natural preproaurelin cDNA using mutagenic PCR primers that substitute rare codons with those preferred by *E. coli* translation system. The plasmid size is 5876 bp. The encoded fusion protein consists of 163 amino acid residues (17.8 kDa). The BL-21 (DE3) cells transformed with pET-His8-TrxL-Aur were grown in LB medium with 100 μg/mL of ampicillin up to OD_{600} 0.8 and then were induced with 0.2 mM isopropyl-β-D-thiogalactopyranoside (IPTG). ^{15}N-labeled aurelin was expressed in M9 minimal medium containing 1 g/L $^{15}NH_4Cl$

(CIL, Andover, MA). Please see experimental details in SI Materials and Methods.

2.2. Recombinant aurelin purification

The cells were harvested by centrifugation and sonicated in the buffer containing 20 mM imidazole. Soluble fraction was separated by centrifugation and then loaded into Ni–NTA column. The recombinant protein was eluted with the buffer containing 0.5 M imidazole. After dialysis the protein of interest was dissolved in 80% TFA and then cleaved by an equal mass of CNBr under standard conditions. The lyophilized products of the cleavage reaction were dissolved in the cell lysis buffer (pH 7.8), and the carrier protein was eliminated from the mix by the second Ni–NTA chromatography stage.

The clarified solution was loaded to the RP-HPLC semi-preparative column Reprosil-pur C18-AQ (Dr. Maisch GmbH) equilibrated with solution A (5% acetonitrile, 0.1% TFA). The chromatography was performed in a step gradient of solution B (80% acetonitrile, 0.1% TFA). The peaks were monitored at 214 nm, collected, vacuum dried, and applied to Tris–tricine SDS–PAGE. Please see experimental details in SI Materials and Methods. TFA was removed during repetitive lyophilization. The purified recombinant aurelin was analyzed by MALDI-TOF MS using Reflex III mass-spectrometer (Bruker Daltonics) and by automated Edman degradation using the Procise cLC 491 Protein Sequencing System (PE Applied Biosystems). The obtained peptide had a purity of at least 99% as measured by RP-HPLC, MALDI-TOF MS, and NMR.

2.3. Antimicrobial assay

Antibacterial activity of the purified aurelin against Gram-positive and Gram-negative bacteria was measured by the radial diffusion assay as described in [19]. Minimal inhibitory concentrations (MICs) of the recombinant peptide were determined using the modified version of the broth microdilution assay [20]. Please see experimental details in SI Materials and Methods.

2.4. NMR experiments, spatial structure calculation and analysis of relaxation data

The NMR investigation was done using 0.5–1.0 mM samples of aurelin or its ^{15}N-labeled analogue in 5% D_2O or 100% D_2O at pH 4.5 and 30 °C. NMR spectra were acquired on a Bruker Avance 600 spectrometer equipped with a cryoprobe. ^{1}H and ^{15}N resonance assignment was obtained by a standard procedure using combination of 2D and 3D TOCSY and NOESY spectra [21]. Spatial structure calculation was performed using the CYANA program [22]. The disulfide bond connectivity pattern was established on the basis of observed NOE contacts and verified during preliminary stages of spatial structure calculation. Backbone dynamics of aurelin in aqueous solution was investigated using ^{15}N-relaxation measurements. R_1 and R_2 relaxation rates and heteronuclear ^{15}N-{^{1}H} NOEs were analyzed using the so-called "model-free" approach (Fig. S5) [21]. Details of experiments and analysis of NMR data are described in SI Materials and Methods.

2.5. Aurelin binding to lipid vesicles and DPC micelles

Small unilamellar vesicles (SUV) were prepared via sonication using POPC or POPC/DOPG (3:1) mixture (Avanti Polar Lipids, Alabaster, AL) in 10 mM Tris–Ac buffer (pH 7.0) with or without 100 mM NaCl. The final lipid concentrations were measured via 1D ^{1}H NMR spectroscopy by dissolving the small fractions of SUV preparation in the $CDCl_3/CD_3OD/D_2O$ (15:10:3) mixture. Titration of ^{15}N-labeled aurelin sample (30 μM, 5% D_2O, same buffer) with SUV was performed at 30 °C. At each lipid concentration, 1D ^{1}H NMR spectrum was measured and the equilibrium concentration of free peptide in solution C_f was determined using the integral intensity of the amide-aromatic region of the spectrum. The binding isotherms were analyzed as a partition equilibrium [23] using the formula:

$$\frac{C_b}{L^*} = K_p \times C_f, \quad C_0 = C_f + C_b \tag{1}$$

where C_b is the bound peptide concentration, C_0 is the total peptide concentration, K_p is the partition coefficient, and L^* is the lipids concentration in the outer leaflet of the vesicles (60% of total lipid, $L^* = 0.6 \times L$). The effect of dilution was accounted for.

The adsorption isotherm of aurelin to the surface of the d38-DPC (CIL) micelle was measured using previously described method [24]. This isotherm was analyzed using partition equilibrium Eq. (1) assuming that L^* is equal to total detergent concentration in the sample. The model of the aurelin–micelle complex was built using lipid-soluble relaxation probe 16-doxylstearate (16-DSA, SIGMA). Please see experimental details in SI Materials and Methods.

3. Results

3.1. Aurelin heterologous expression, purification and characterization

In order to achieve a higher yield of a soluble aurelin expressed in *E. coli* cytoplasm, thus avoiding the refolding procedure after the peptide isolation from inclusion bodies, the amino acid sequence of the peptide was fused with His-tagged thioredoxin carrier protein as described [25]. Cyanogen bromide cleavage at the single methionine inserted downstream of the carrier protein allowed to produce an exact analogue of the natural peptide lacking any additional residues. The target gene was placed under control of T7lac promoter within a low copy number plasmid that was introduced into *E. coli* BL21(DE3) strain, and the expression was induced by IPTG. The purification protocol consisted of the cell harvesting, sonication and preparative centrifugation of the cell lysate, immobilized metal ion affinity chromatography (IMAC) of the fusion protein, dialysis against acetic acid solution, cyanogen bromide cleavage of the fusion protein, elimination of the carrier protein by the second round of IMAC, and fine aurelin purification using reversed-phase HPLC in acetonitrile concentration gradient.

In LB medium the recombinant protein was obtained mostly in a soluble form. The yield constituted up to 3.5 mg/L of the medium (in conversion to pure peptide). In M9 minimal medium the yield of ^{15}N-labeled recombinant protein was somewhat lower (2.5 mg/L), mostly due to the fact that about half of the fusion protein was deposited in inclusion bodies.

The recombinant peptide and its ^{15}N-labeled analogue were characterized by SDS–PAGE, MALDI-TOF mass spectrometry, automated microsequencing, and antimicrobial activity testing. The unlabeled recombinant aurelin was proved to be identical to the natural peptide in respect of its molecular mass (4296.4 Da) and amino acid sequence. The ^{15}N-labeled aurelin analogue showed 60 Da increase in molecular mass (4356.6 Da) indicating that all the ^{14}N atoms were substituted with stable isotope ^{15}N.

3.2. Biological activity of recombinant aurelin

Antimicrobial activity of the recombinant aurelin was examined by the radial diffusion assay against eight test microorganisms, including Gram-positive and Gram-negative bacteria (Fig. 2). Aurelin was active against all the test microorganisms, but at rather high inhibitory concentrations. Minimal inhibitory concentrations

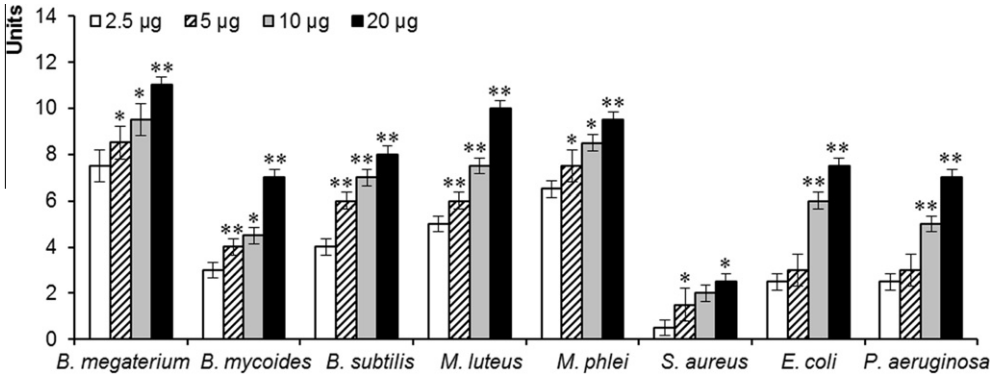

Fig. 2. Antimicrobial activity of aurelin. Data shown are mean ±SEM of five independent experiments performed in duplicate. $^{*}P \leqslant 0.05$; $^{**}P < 0.005$, indicate statistically significant differences between different peptide concentrations.

(MICs) were determined using the broth microdilution assay for the most aurelin-sensitive test microorganisms – the *Bacillus megaterium*, strain B-392, and the *Micrococcus luteus*, strain Ac-2229 (the MICs of 10 and 40 μM, respectively).

3.3. Spatial structure and ionization properties of aurelin in aqueous solution

The spatial structure of aurelin was studied by $^{1}H–^{15}N$ NMR spectroscopy in aqueous solution at pH 4.5 (Fig. 3A). The summary of the obtained NMR data, a calculated set of 20 structures, and structural statistics are shown in Fig. S2 and Table S1, respectively. The peptide (Fig. 4A) represents a compact globule cross-linked by three disulfide bonds (Cys3-Cys40, Cys12-Cys33, and Cys19-Cys37). The secondary structure of aurelin involves two helical regions. The fist of them (His10-Asp21) is divided into α-helix (His10-Phe15) and 3_{10}-helix (Lys16-Asp21) by the ~60° kink at Phe15. The second region (Arg24-Asn32) has an α-helical conformation. The aurelin structure is stabilized by 17 backbone–backbone hydrogen bonds. The maps of electrostatic (Fig. 4B) and molecular hydrophobicity (Fig. 4C) potentials revealed the pronounced hydrophobic patch on the otherwise positively charged surface of aurelin (net charge +7). This patch formed by the side chains of Ile11, Phe15, and Phe18 endows the peptide structure with the moderate amphipathicity.

The pH dependence of the peptide chemical shifts and $^{3}J_{H^{N}H^{\alpha}}$ coupling constants was monitored in the range from 2.0 to 6.0. The analysis of pH titration curves allowed to measure the pK_a values for the side chains of Asp5, Glu13, Asp21, and C-terminal carboxyl group (2.8, 3.8, 3.0, and 2.6, respectively). The pKa values for His8 and His10 side chains were estimated to be above 5.5. The precise determination of His pKa was impossible due to significant broadening of His resonances observed at higher pH. Thus, at pH 4.5 used for structural study all acidic groups and His side chains of the peptide were almost fully charged. Comparison of the $^{3}J_{H^{N}H^{\alpha}}$ values measured at pH 3.2, 4.5 and 6.0 (Fig. S3A) did not reveal significant pH-induced changes in the conformation of the aurelin backbone. This indicates that the peptide has quite similar spatial structure at acidic and neutral pH.

The pH titration also did not reveal notable changes of the Arg and Lys side chain chemical shifts upon changes in ionization state of the carboxylic groups. This points to the absence of salt-bridge interactions between positively and negatively charged residues within the peptide. The analysis of pH titration curve for the H^{N} proton of Thr36 (Fig. S4) reveals the formation of a hydrogen bond with Asp5 carboxyl group (Fig. 4A). Together with Cys3-Cys40 disulfide bridge, this hydrogen bond controls relative position of the *N*- and *C*-terminal peptide regions.

3.4. Comparison of spatial structures of aurelin, sea anemone toxins and other proteins containing ShKT domain

The obtained results revealed structural homology between aurelin and sea anemone toxins BgK and ShK (Fig. 1B). The peptides share identical disulfide pairing scheme (C1–C6, C2–C4, C3–C5) and secondary structure composed of three helical elements. Nevertheless, the relative orientation and length of these helices are remarkable different. The peptides have quite similar spatial position of the putative "pore blocking" Lys28 side chain (the residue numbers are given for aurelin) relative to the frame of conserved disulfide bonds (RMSD of the aurelin structure from BgK and ShK structures calculated over C^{α} atoms of six Cys and Lys28 is 1.68 and 1.39 Å, respectively). At the same time, the side chain of the second putative "functional dyad" member (Leu29) became buried within the hydrophobic core of the aurelin structure (Fig. 4A and C).

Using C^{α} atoms of the six conserved cysteines, aurelin can also be fairly good superimposed (RMSD in the range from 1.0 to 2.1 Å) with the ShKT domains from various proteins, including rat MMP23, CRISPs from snake venoms (pseudechetoxin, pseudecin, stecrisp, triflin, and natrin), and mouse CRISP-2 (pdb codes: 2K72, 2DDA, 2DDB, 1RC9, 1WVR, 1XTA, and 2A05, respectively). The presence of electrostatic interactions between Asp5 and Lys35-Thr36 residues additionally emphasizes the structural homology between aurelin and other proteins containing ShKT domain. Indeed, these residues are absolutely conserved in sea anemone toxins (Fig. 1A) and important for proper folding of BgK and ShK [10,13]. Moreover, formation of the salt-bridge between carboxyl group of aspartate and ε-amino group of lysine was suggested in the NMR study of ShK [26]. The homologous Asp/Asn...-...Lys/Arg-Thr/Ser motif (in some cases without positively charged Lys/Arg residue) was found in the other ShKT domains (Fig. 1A, arrows). Analysis of the known spatial structures revealed that in majority of cases the conserved Asp (Asn in CRISPs from reptile venoms) could form either hydrogen bond with HN group of the conserved Thr/Ser or salt bridge with the preceding Lys/Arg. Such electrostatic interactions should be manifested in the significant down-field shift of the Thr/Ser amide proton. Indeed, in all the ShKT domains studied by NMR spectroscopy (ShK [11,26], BgK [10], rat MMP23-TxD [16], ICR from mouse CRISP-2 [17], and aurelin) the corresponding $^{1}H^{N}$ resonance was observed with chemical shift above 10 ppm.

3.5. Interaction of aurelin with lipid vesicles

Aurelin binding to differently charged lipid vesicles was studied by NMR spectroscopy. The zwitterionic (POPC) and partially

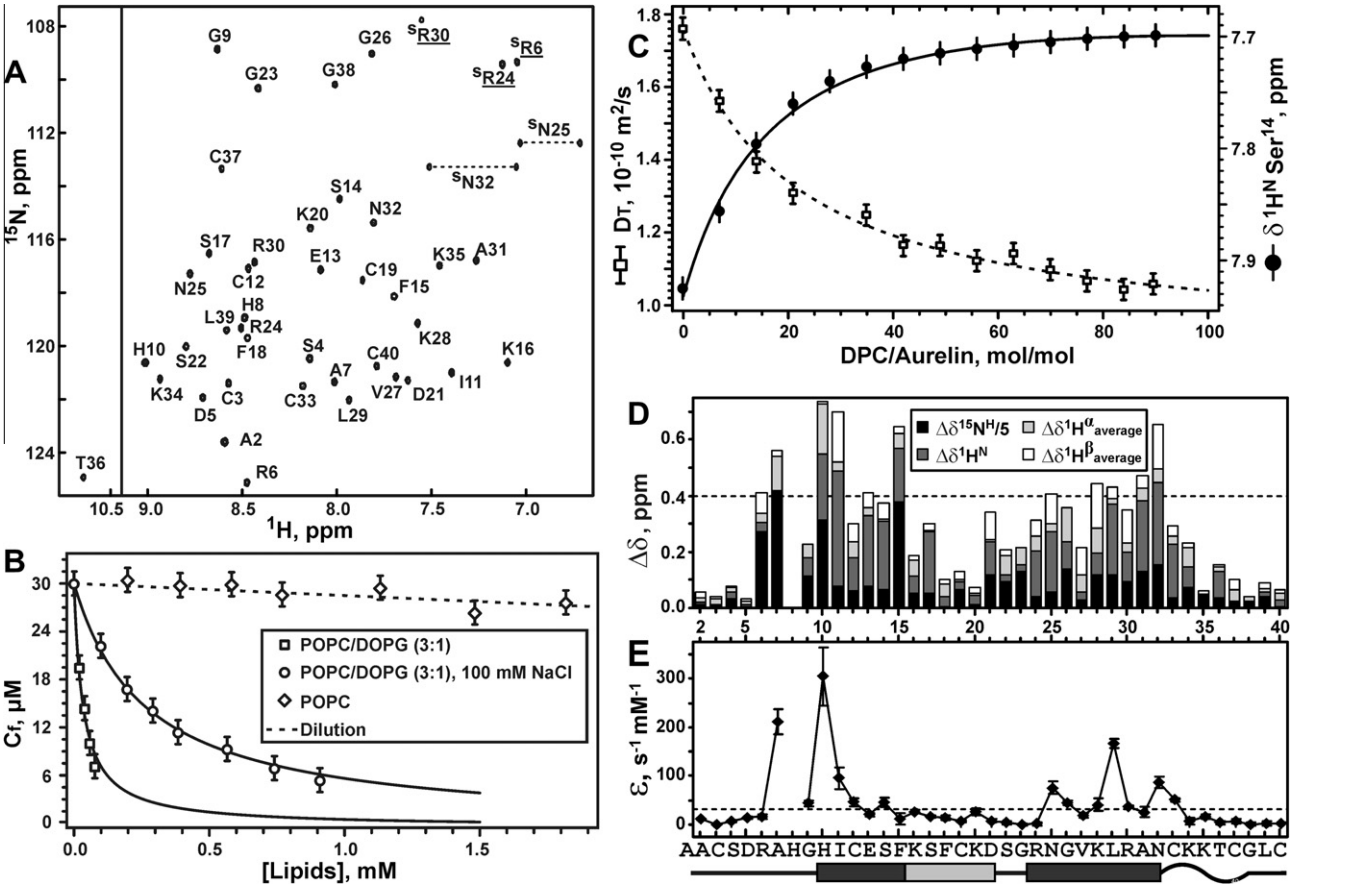

Fig. 3. (A) 2D ^{1}H, ^{15}N-HSQC spectrum of aurelin (0.5 mM, pH 4.5, 30 °C). The obtained resonance assignments are shown. The resonances of side chain groups are marked with superscript "s". The resonances of Asn NH_2 groups are connected by dotted lines. The "folded" resonances are underlined. (B) Isotherms of aurelin binding to POPC, POPC/DOPG (3:1), and POPC/DOPG (3:1, 100 mM NaCl) vesicles are approximated by the partition equilibrium equation. The dilution curve is shown by dashed line. (C) Titration of the 0.5 mM aurelin sample with DPC, pH 4.5, 25 °C. Chemical shift (δ) of the H^N proton of Ser14 (filled circles) and translation diffusion coefficient (D_T) of the aurelin molecule (open squares) are shown versus the DPC/aurelin molar ratio. Chemical shift dependence is approximated by the partition equilibrium equation (solid line). The D_T approximating dashed line is drawn only to guide the eye. (D) Changes of aurelin chemical shifts ($\Delta\delta$) upon incorporation into the DPC micelle. The 0.4 ppm threshold line marks out the residues, which are in contact with the micelle. (E) Paramagnetic enhancement (ε) of the H^N proton R_2 relaxation induced by lipid-soluble 16-DSA. The 30 s^{-1} mM^{-1} threshold line subdivides data points in two groups: the residues located inside or outside the hydrophobic region of the micelle. H^N proton of His8 was unobservable in DPC micelles solution at pH 4.5.

anionic (POPC/DOPG 3:1) lipid vesicles were used to model membranes of eukaryotic and bacterial cells, respectively. Titration of the peptide sample with the POPC/DOPG SUV led to the gradual decrease of the aurelin NMR signal intensity (Fig. S6). The observed attenuation could be explained by tight association of the peptide molecules with the vesicle surface. In this case, due to very slow reorientation of the SUV in solution, the bound peptide molecules become unobservable by high-resolution NMR spectroscopy and the intensity of NMR signal is directly proportional to the equilibrium concentration of the free peptide in solution (C_f). Analysis of the measured binding isotherm revealed effective partitioning of aurelin into the partially anionic SUV with the partition coefficient K_p equal to $50 \pm 4 \times 10^3$ M^{-1} (Fig. 3B). Addition of the 100 mM NaCl into the binding buffer significantly diminished the peptide affinity to the POPC/DOPG SUV, but did not abolish it completely ($K_p = 6.3 \pm 0.2 \times 10^3$ M^{-1}). Probably, electrostatic interactions play the major role in the peptide/lipid binding. This conclusion is also supported by the absence of delectable aurelin interaction with the zwitterionic POPC vesicles (Fig. 3B).

Efficiency of the observed aurelin partitioning into the negatively charged lipid vesicles was lower than one reported previously for other cationic AMPs from sea invertebrates. For example, the β-hairpin peptides polyphemusins isolated from horseshoe crab interact with POPC/POPG SUV (3:1, 150 mM NaCl) with K_p values in a range of $30–50 \times 10^3$ M^{-1} [23]. At the same time, absence of interactions with uncharged membranes is quite typical for cationic AMPs. No binding to the POPC vesicles was detected for β-hairpin peptide arenicin isolated from marine polychaeta *Arenicola marina* [25,27], and very weak binding ($K_p \sim 1–3 \times 10^3$ M^{-1}) was observed for polyphemusins [23].

3.6. Interaction of aurelin with DPC micelles

To characterize the membrane bound conformation of aurelin the DPC micelles were chosen as the membrane-mimicking environment. Formation of the complex between aurelin and the DPC micelle was studied using diffusion measurements and ^{1}H–^{15}N NMR spectroscopy at 25 °C. The chemical shifts of several signals of the peptide were affected by variation of the detergent to peptide molar ratio (D:P) (Fig. 3C and D). In the limit of fast exchange between bound and free peptide species, the value of chemical shift of the affected proton simply reflects the fraction of the bound peptide at a given D:P. The changes in chemical shift of the H^N proton of Ser14 (which is located close to the hydrophobic region of the peptide) revealed that the peptide became fully micelle-bound at D:P above 80:1 (Fig. 3C). Analysis of this binding curve using the partition equilibrium equation revealed that the peptide has relatively low affinity to the micelle surface ($K_p = 0.97 \pm 0.01 \times 10^3$ M^{-1}).

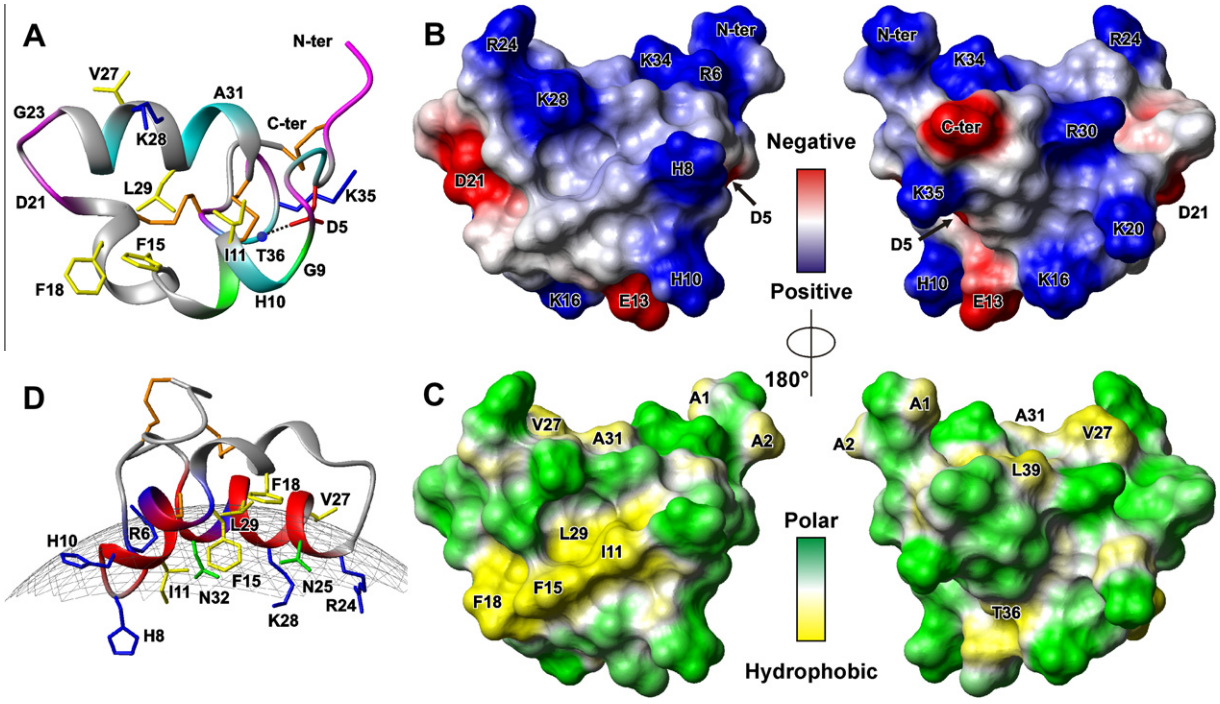

Fig. 4. (A) Spatial structure and backbone dynamics of aurelin in aqueous solution. The peptide ribbon is colored according to the dynamical NMR data obtained from the ^{15}N-relaxation measurements. The residues affected by dynamic processes on the picosecond to nanosecond time scale (one with generalized order parameter $S^2 < 0.7$ or demonstrating nanosecond motions) are shown in magenta. The residues affected by dynamic processes on the microsecond to millisecond time scale (having exchange contribution R_{EX} to the R_2 relaxation rate of ^{15}N nuclei) are shown in cyan. The residues demonstrating mobility on both time scales are in green. The backbone amide of Thr36 and hydrogen bond H^N Thr36 – $O^{\delta1}$ Asp5 are shown by blue sphere and dotted line. (B and C) Two-sided view of electrostatic and molecular hydrophobicity potentials on the aurelin surface. (D) The model of aurelin/DPC micelle complex. The peptide ribbon is colored according to experimental data presented on the (Fig. 3D and E). The residues located inside the micelle according to 16-DSA paramagnetic relaxation enhancement data are colored in red. The residues which according to chemical shift perturbation data are in contact with the micelle, are colored in blue. The approximate micelle surface ($R \sim 23$ Å) is shown as a gray mesh. In (A and D) the disulfide bonds, positively charged, negatively charged, hydrophobic/aromatic, and other polar residues are colored in orange, blue, red, yellow, and green, respectively. (For interpretation of the references to colour in this figure legend, the reader is referred to the web version of this article.)

The translational diffusion coefficient of aurelin also showed a gradual decrease upon increasing detergent content in the sample (Fig. 3C), thus indicating formation of the aurelin/DPC complexes. The diffusion coefficient of the peptide in a complex with DPC micelle ($1.04 \pm 0.03 \times 10^{-10}$ m^2 s^{-1}, D:P = 90:1, 25 °C) corresponds to a hydrodynamic Stokes radius of 23.5 ± 0.6 Å. Thus, the aurelin/DPC complex has dimensions similar to the pure DPC micelle ($R_H \sim 23.1 \pm 0.5$ Å [24]). Comparison of the $^3J_{H^NH^\alpha}$ coupling constants and temperature coefficients of amide protons (Fig. S3) did not reveal considerable changes in the conformation of the aurelin backbone upon incorporation into DPC micelle.

The topology of the aurelin/DPC complex was elucidated using lipid-soluble relaxation probe 16-DSA with the paramagnetic nitroxide moiety being preferentially located close to the micelle center [24]. The paramagnetic relaxation enhancement (ε) induced by 16-DSA revealed that the two regions of the peptide are embedded into the micelle interior (Fig. 3E). These regions (Ala7-Ser14 and Gln25-Cys33) involve the two α-helices and coincide with the sites where largest DPC-induced chemical shift changes were observed (Fig. 3D). Interestingly, the relaxation enhancement in these regions has a remarkable helical (i, $i+4$ or i, $i+3$) periodicity and the H^N protons of Ala7, His10, Asn25, Leu29, and Asn32 demonstrated largest increase in the R_2 relaxation rates (Fig. 3E). In the obtained model of the aurelin/DPC complex (Fig. 4D), the peptide interacts with the surface of DPC micelle by two α-helical regions; and the hydrophobic side chains of Ile11, Phe15, Val27, and Leu29 are located at the binding interface. At the same time the positively charged side chains of Arg6, His8, His10, Arg24, and Lys28 either protrude into the micelle interior or reside in close proximity to its surface.

4. Discussion

Membrane-active antimicrobial peptides and the toxins represent two broad and evolutionally ancient peptide families [1–3,7]. These molecules have different targets (the membranes of microorganisms *vs.* membrane receptors of eukaryotic cells), and different interactions underlie their activity (semi-specific peptide/lipid *vs.* highly specific protein/protein interactions) [4–6,8]. In spite of this, the peptides from both families could share common structural and biochemical properties, including molecular scaffold, cationicity, amphipathicity, resistance to enzymatic hydrolysis, and overall compactness.

The determined spatial structure of aurelin did not reveal homology to any previously identified antimicrobial peptides, but displayed close similarity to the structure of the K^+-channel blocking toxins from sea anemones (BgK and ShK) (Fig. 1). In spite of this similarity, the surface of the aurelin molecule does not possess the "functional dyad" element required for the high-affinity toxin binding to the external vestibule of Kv channels [8,10]. Indeed, aurelin demonstrates quite similar spatial position of the "pore blocking" Lys28, but the side chain of the second putative dyad member Leu29 became deeply buried within the aurelin interior (Fig. 4C). The obtained results permit to propose that aurelin is not a K^+-channel blocker.

Despite large structural diversity, the membrane-active AMPs have common properties essential for their activity, e.g., amphipathicity and overall positive charge needed for the efficient, but low-specific, interactions with anionic bacterial membranes [1,4–6]. According to the presently obtained data, aurelin (net charge +7) has structural properties typical for membrane-active AMPs.

Indeed, the modest antibacterial activity of aurelin against Gram-positive and Gram-negative organisms (Fig. 2) could be correlated with the amphipathic properties of its structure (Fig. 4C) and with the observed moderate affinity to the negatively charged (POPC/DOPG 3:1) lipid vesicles (Fig. 3B). The absence of the detectable aurelin interaction with the zwitterionic (POPC) lipid vesicles, which model membranes of eukaryotic cells, could be explained on the ground of the determined structure of the aurelin/DPC micelle complex (Fig. 4D). The positively charged side chains of Arg6, His8, His10, Arg24, and Lys28 protrude into the hydrophobic "micelle binding" interface of the peptide. These side chains probably prevent aurelin binding to the uncharged (zwitterionic) lipid bilayers, but promote interaction with the anionic membranes by formation of favorable contacts with the negatively charged lipids. Aurelin binding to the POPC/DOPG vesicles observed at 100 mM NaCl indicates that the peptide can possess affinity to bacterial membranes at physiological conditions. At the same time, as shown in many studies of membrane-active AMPs [1,28,29], the accumulation of the peptide molecules in the outer leaflet of the membrane diminishes its stability and eventually leads to the bilayer disruption. Thus, we could speculate that the observed antimicrobial activity of aurelin is membrane-mediated and conditioned by electrostatic interactions with the membranes of bacterial cells. Interestingly, the determined site of aurelin interaction with DPC micelle (Fig. 4D) almost completely coincides with the channel binding interface of BgK and ShK toxins (Fig. 1B). This could be a consequence of a divergent character of evolution of these molecules.

In summary, although the possible aurelin action on the membrane receptors/ionic channels could not be presently ruled out, we can conclude that aurelin represents the first antimicrobial having the ShKT fold. The observed conservation of the ShKT domain in different animals from coelenterates to mammals [12,15–18] verifies its ancient origin and ability to establish multiple biological functions including channels blocking, antimicrobial activity, and perhaps other currently unknown properties.

Acknowledgments

This work was supported by the Federal Target Program "Scientific and Science-Educational Personnel of Innovative Russia" (state contracts P1159, 8789, and 8043) and by Russian Academy of Sciences (the Program "Molecular and Cellular Biology").

Appendix A. Supplementary data

Supplementary data associated with this article can be found, in the online version, at http://dx.doi.org/10.1016/j.bbrc.2012.10.092.

References

[1] P. Bulet, R. Stöcklin, L. Menin, Anti-microbial peptides: from invertebrates to vertebrates, Immunol. Rev. 198 (2004) 169–184.
[2] J.A. Tincu, S.W. Taylor, Antimicrobial peptides from marine invertebrates, Antimicrob. Agents Chemother. 48 (2004) 3645–3654.
[3] S.V. Sperstad, T. Haug, H.M. Blencke, O.B. Styrvold, C. Li, K. Stensvåg, Antimicrobial peptides from marine invertebrates: challenges and perspectives in marine antimicrobial peptide discovery, Biotechnol. Adv. 29 (2011) 519–530.
[4] R.J. Pieters, C.J. Arnusch, E. Breukink, Membrane permeabilization by multivalent anti-microbial peptides, Protein Pept. Lett. 16 (2009) 736–742.
[5] V. Teixeira, M.J. Feio, M. Bastos, Role of lipids in the interaction of antimicrobial peptides with membranes, Protein Pept. Lett. 51 (2012) 149–177.
[6] J.P. Tam, Y.-A. Lu, J.-L. Yang, Correlations of cationic charges with salt sensitivity and microbial specificity of cystine-stabilized β-strand antimicrobial peptides, J. Biol. Chem. 277 (2002) 50450–50456.
[7] N. Fusetani, W. Kem, Marine toxins: an overview, Prog. Mol. Subcell Biol. 46 (2009) 1–44.
[8] B. Jouirou, S. Mouhat, N. Andreotti, M. De Waard, J.M. Sabatier, Toxin determinants required for interaction with voltage-gated K^+-channels, Toxicon 43 (2004) 909–914.
[9] T.V. Ovchinnikova, S.V. Balandin, G.M. Aleshina, A.A. Tagaev, Y.F. Leonova, E.G. Krasnodembsky, A.V. Men'shenin, V.N. Kokryakov, Aurelin, a novel antimicrobial peptide from jellyfish *Aurelia aurita* with structural features of defensins and channel-blocking toxins, Biochem. Biophys. Res. Commun. 348 (2006) 514–523.
[10] M. Dauplais, A. Lecoq, J. Song, J. Cotton, N. Jamin, B. Gilquin, C. Roumestand, C. Vita, C.L. de Medeiros, E.G. Rowan, A.L. Harvey, A. Ménez, On the convergent evolution of animal toxins. Conservation of a diad of functional residues in potassium channel-blocking toxins with unrelated structures, J. Biol. Chem. 272 (1997) 4302–4309.
[11] J.E. Tudor, P.K. Pallaghy, M.W. Pennington, R.S. Norton, Solution structure of ShK toxin, a novel potassium channel inhibitor from a sea anemone, Nat. Struct. Biol. 3 (1996) 317–320.
[12] R.S. Norton, Structures of sea anemone toxins, Toxicon 54 (2009) 1075–1088.
[13] M.W. Pennington, V.M. Mahnir, I. Khaytin, I. Zaydenberg, M.E. Byrnes, W.R. Kem, An essential binding surface for ShK toxin interaction with rat brain potassium channels, Biochemistry 35 (1996) 16407–16411.
[14] B. Gilquin, J. Racapé, A. Wrisch, V. Visan, A. Lecoq, S. Grissmer, A. Ménez, S. Gasparini, Structure of the BgK-Kv1.1 complex based on distance restraints identified by double mutant cycles. Molecular basis for convergent evolution of Kv1 channel blockers, J. Biol. Chem. 277 (2002) 37406–37413.
[15] A. Loukas, M. Hintz, D. Linder, N.P. Mullin, J. Parkinson, K.K. Tetteh, R.M. Maizels, A family of secreted mucins from the parasitic nematode *Toxocara canis* bears diverse mucin domains but shares similar flanking six-cysteine repeat motifs, J. Biol. Chem. 275 (2000) 39600–39607.
[16] S. Rangaraju, K.K. Khoo, Z.P. Feng, G. Crossley, D. Nugent, I. Khaytin, V. Chi, C. Pham, P. Calabresi, M.W. Pennington, R.S. Norton, K.G. Chandy, Potassium channel modulation by a toxin domain in matrix metalloprotease 23, J. Biol. Chem. 285 (2010) 9124–9136.
[17] G.M. Gibbs, M.J. Scanlon, J. Swarbrick, S. Curtis, E. Gallant, A.F. Dulhunty, M.K. O'Bryan, The cysteine-rich secretory protein domain of Tpx-1 is related to ion channel toxins and regulates ryanodine receptor Ca^{2+} signaling, J. Biol. Chem. 281 (2006) 4156–4163.
[18] Y. Yamazaki, T. Morita, Structure and function of snake venom cysteine-rich secretory proteins, Toxicon 44 (2004) 227–231.
[19] R.I. Lehrer, M. Rosenman, S.S. Harwig, R. Jackson, P. Eisenhauer, Ultrasensitive assays for endogenous antimicrobial polypeptides, J. Immunol. Methods 137 (1991) 167–173.
[20] C.B. Park, K.S. Yi, K. Matsuzaki, M.S. Kim, S.C. Kim, Structure-activity analysis of buforin II, a histone H2A-derived antimicrobial peptide: the proline hinge is responsible for the cell-penetrating ability of buforin II, Proc. Natl. Acad. Sci. 97 (2000) 8245–8250.
[21] G.S. Rule, K.T. Hitchens, Fundamentals of Protein NMR Spectroscopy, Springer, Netherlands, 2006.
[22] P. Guntert, Automated NMR structure calculation with CYANA, Method Mol. Biol. 278 (2004) 353–378.
[23] J.P. Powers, A. Tan, A. Ramamoorthy, R.E. Hancock, Solution structure and interaction of the antimicrobial polyphemusins with lipid membranes, Biochemistry 44 (2005) 15504–15513.
[24] Z.O. Shenkarev, K.D. Nadezhdin, V.A. Sobol, A.G. Sobol, L. Skjeldal, A.S. Arseniev, Conformation and mode of membrane interaction in cyclotides. Spatial structure of kalata B1 bound to a dodecylphosphocholine micelle, FEBS J. 273 (2006) 2658–2672.
[25] T.V. Ovchinnikova, Z.O. Shenkarev, K.D. Nadezhdin, S.V. Balandin, M.N. Zhmak, I.A. Kudelina, E.I. Finkina, V.N. Kokryakov, A.S. Arseniev, Recombinant expression, synthesis, purification, and solution structure of arenicin, Biochem. Biophys. Res. Commun. 360 (2007) 156–162.
[26] J.E. Tudor, M.W. Pennington, R.S. Norton, Ionisation behaviour and solution properties of the potassium-channel blocker ShK toxin, Eur. J. Biochem. 251 (1998) 133–141.
[27] Z.O. Shenkarev, S.V. Balandin, K.I. Trunov, A.S. Paramonov, S.V. Sukhanov, L.I. Barsukov, A.S. Arseniev, T.V. Ovchinnikova, Molecular mechanism of action of β-hairpin antimicrobial peptide arenicin: oligomeric structure in dodecylphosphocholine micelles and pore formation in planar lipid bilayers, Biochemistry 50 (2011) 6255–6265.
[28] H.W. Huang, Molecular mechanism of antimicrobial peptides: the origin of cooperativity, Biochim. Biophys. Acta 1758 (2006) 1292–1302.
[29] Y. Shai, Mechanism of the binding, insertion and destabilization of phospholipid bilayer membranes by alpha-helical antimicrobial and cell non-selective membrane-lytic peptides, Biochim. Biophys. Acta 1462 (1999) 55–70.